

Tuneable electron-beam-driven nanoscale light source

G Adamo^{1,4}, K F MacDonald¹, Y H Fu², D P Tsai²,
F J García de Abajo³ and N I Zheludev¹

¹ Optoelectronics Research Centre, University of Southampton, Highfield, Southampton SO17 1BJ, UK

² Department of Physics, National Taiwan University, Taipei 10617, Taiwan, Republic of China

³ Instituto de Óptica—CSIC, Serrano 121, 28006 Madrid, Spain

E-mail: gia@orc.soton.ac.uk

Received 27 July 2009, accepted for publication 30 September 2009

Published 11 January 2010

Online at stacks.iop.org/JOpt/12/024012

Abstract

Recently demonstrated ‘light-wells’—free-electron-driven tuneable nanoscale light sources—generate optical photons as electrons travel down a nano-hole through a metal–dielectric multilayer structure. We report here on the application of boundary element modeling methods to the simulation of light-well output characteristics. The model is found to successfully reproduce the key features observed in experiment and as such will aid in the development and optimization of future device structures.

Keywords: free-electron, light source, tuneable, nanoscale emitter

(Some figures in this article are in colour only in the electronic version)

It is widely recognized that the future advancement of technology will depend critically on whether the current trend for the miniaturization of sophisticated devices can be sustained. Indeed, multi-billion dollar initiatives around the world, such as the USA’s National Nanotechnology Initiative [1], currently give the highest priority to research on fundamental nanoscale phenomena and nanomaterials. With this in mind, and with ongoing rapid developments in the technology of chip-scale free-electron sources making highly integrated chip-scale free-electron devices a realistic possibility [2], there is growing interest in the opportunities presented by new phenomena and functionalities found at the interface between nanophotonics (including plasmonics) and electron beam optics in nanostructured media. In such applications, the primary attraction of free electrons is the fact that they can be focused and positionally controlled on the nanometer scale—far below the diffraction limit of light. An electron beam can, for example, act as a highly localized source of surface plasmon–polaritons on unstructured metal surfaces [3, 4] (enabling high-resolution mapping of plasmonic modes in nanostructures [5–7]), or as an excitation source

for selective switching of phase-change memory elements (presenting the possibility of terabit-per-square-inch data storage densities [8]).

Most recently, the experimental demonstration of a new, nanoscale, electron-beam-driven emitter—the ‘light-well’—has been reported [9, 10]. In a light-well, optical photons are generated as free electrons travel through a hole in a layered metal–dielectric structure, with emission wavelength being a strong function of incident electron energy. Light-wells have the notable advantage (over many other kinds of nanoscale emitter [11–15]) of being dynamically tuneable. Here, we consider the complex combination of material and geometry-dependent mechanisms contributing to the light-well emission process, and employ boundary element numerical techniques to model the emission characteristics.

Reference [10] reported on experimental light-wells with a diameter of 750 nm milled through a stack of eleven 200 nm gold and silica layers (figures 1(a) and (b)), pumped at electron energies between 20 and 40 keV. The experimental findings can be summarized as follows.

- The light-well emission spectrum contains two distinct peaks (I and II in figure 1(c)) at wavelengths that blue-shift strongly with increasing electron energy (see upper

⁴ www.nanophotonics.org.uk/niz.

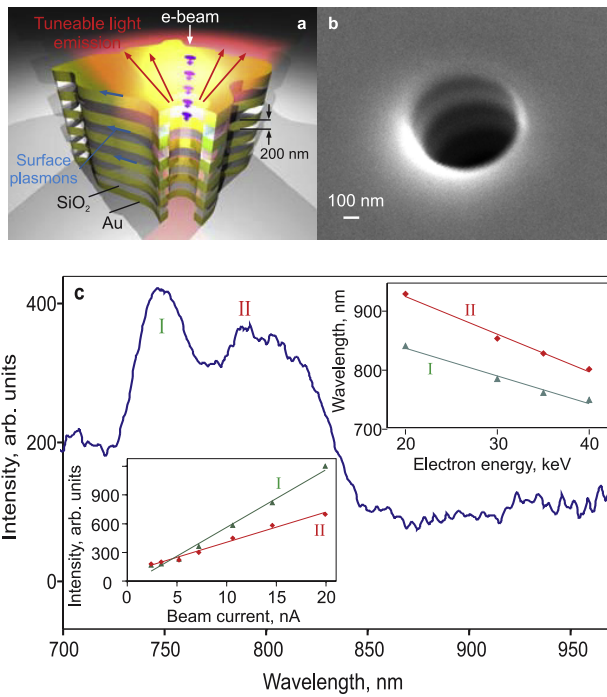


Figure 1. (a) Artist's impression of a light-well: light is emitted as electrons are launched into a nano-hole through a metal–dielectric multilayer structure. (b) Scanning electron microscope image of a gold–silica light-well as studied in [10]. (c) Emission spectrum from a 750 nm diameter well pumped by 40 keV electrons injected ~ 100 nm inside the wall of the well. The upper right inset shows the spectral position of peaks I and II as a function of electron energy. The lower left inset shows that the emission intensity into each peak as a function of electron beam current for an electron energy of 40 keV and an injection point ~ 100 nm from the light-well wall.

right inset to figure 1(c)). (Electron impact on the sample surface outside the well generates cathodoluminescent emission (including transition radiation) characteristic of the materials present in the structure, i.e. gold and silica. The spectrum of this emission does *not* change with electron energy.)

- These peaks are visible for electron injection points within ~ 200 nm of the light-well wall; emission intensity increases with the proximity of the injection point to the wall.
- For a fixed electron injection point and energy, the emission intensity increases linearly with electron beam current (lower left inset to figure 1(c)). (A maximum emission efficiency around the peak wavelengths of 3.4×10^{-5} photons/electron (an emission intensity of ~ 200 W cm $^{-2}$) was recorded.)

As discussed in [10], analytical approximations provide some insight into the light-well emission process: the inverse proportionality between electron energy and emission wavelength emerges from the basic assumption that electrons passing down the well form oscillating dipoles with their ‘mirror images’ in the wall; the increased emission probability for injection points closer to the wall can be expressed in terms of a modified Bessel function describing the strength of the electron–wall interaction; and the complexity of

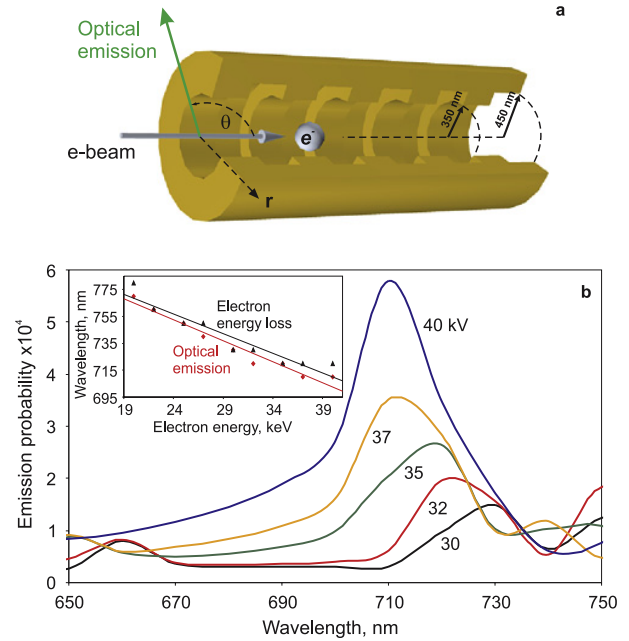


Figure 2. (a) Light-well structure modeled using the boundary element method: a solid gold well with an internal rectangular grating profile of max./min. internal radius 450/350 nm and external radius 2350 nm; period = 400 nm; number of periods $n = 6$ unless otherwise stated. Emission zenith angle θ is measured relative to the direction of electron propagation: i.e. 0° = parallel, 180° = antiparallel. (b) Optical emission probability (photons per electron integrated over angles θ from 100° to 180°) as a function of emission wavelength for electrons with a range of energies (as labeled) injected at a radial distance $r = 300$ nm. The inset shows the spectral positions of emission probability and electron energy loss peaks as a function of incident electron energy.

the well’s guided photonic mode profile (multiple emission wavelengths for a given electron energy) is illustrated by the dispersion diagram for a periodic cylindrical cavity. However, a single analytical model cannot account for the complex interplay between material- and geometry-dependent emission mechanisms (dipole oscillation, surface plasmon excitation and scattering) and light-guiding characteristics (along the well axis and within the dielectric layers). Numerical methods provide an alternative approach to the interpretation of experimental results and to the design process for improved light-well structures.

Indeed, the boundary element method (BEM), which solves Maxwell’s equations in frequency space and calculates the scattered electromagnetic fields expressed in terms of boundary charges and currents discretized at representative points [16, 17], has been established as a powerful tool for the analysis of free-electron interactions with, and the optical/plasmonic properties of nanostructures [7, 18]. In the particular case of the light-well, the layered structure incorporating optically transparent material presents a computational problem: despite the fact that the axially symmetric well can be defined by a two-dimensional cross-section, the number of points required to define these layers to a sufficient radial distance is prohibitive (to a first approximation, computational time scales as N^3 , where N

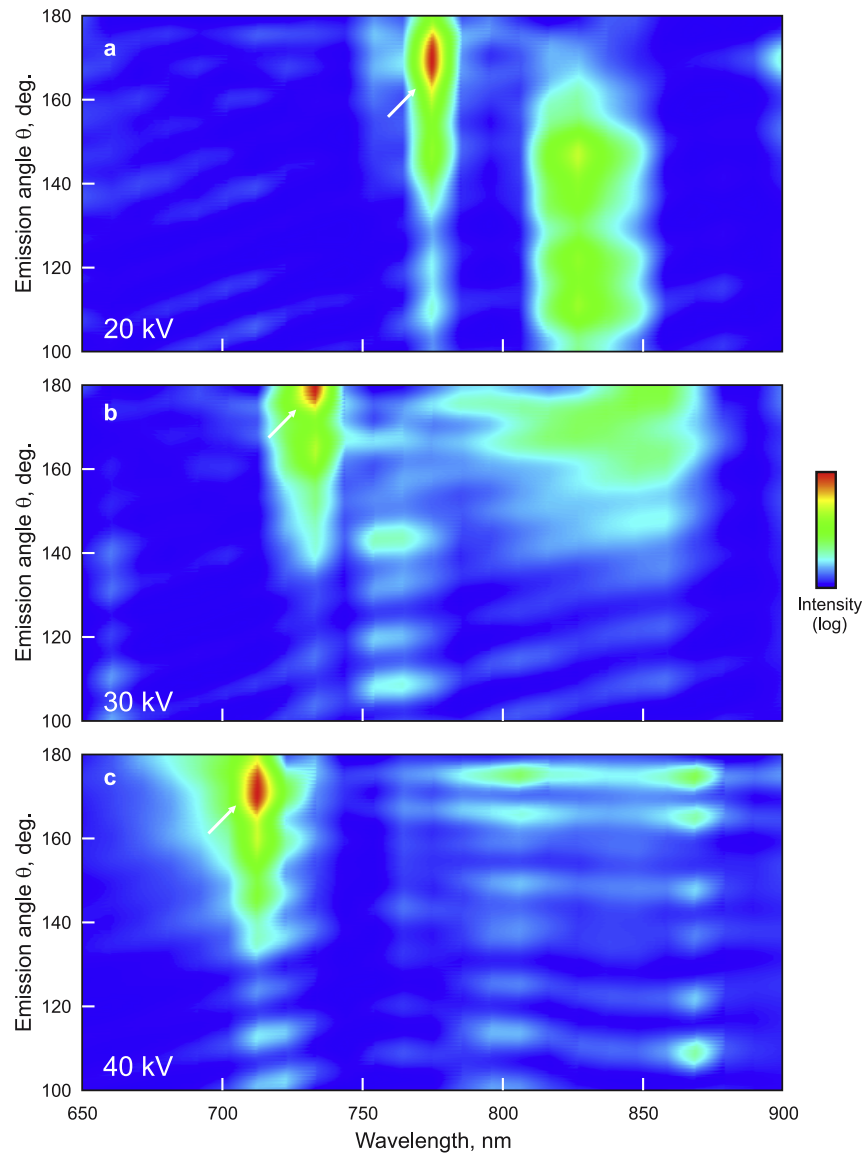


Figure 3. Emission probability as a function of wavelength and emission angle θ (as defined in figure 2(a)) for 20, 30 and 40 keV electrons injected into the well geometry defined in figure 2(a) at $r = 300$ nm. ((a)–(c) are separately normalized; the maxima in (b) and (c) being respectively 2.4 and 6.8 times the maximum in (a).)

is the number of points). Thus, to allow for the impact of variations in individual structural and operational parameters to be studied, in what follows we consider a solid gold light-well with a corrugated internal profile (see figure 2(a)) as opposed to a smooth-walled gold–silica structure.

In the first instance, this model clearly reproduces the blue-shift in emission wavelength that is observed with increasing electron energy (figure 2(b)). Furthermore, in evaluating emission probability, the BEM also determines electron energy loss during propagation resulting from interaction with nearby structures. In the case of the light-well, as shown by the inset to figure 2(b), such calculations reveal a clear correlation between peaks in the emission and electron energy loss spectra. A more detailed picture of the emission profile is provided by angle-resolved plots of emission probability such as those presented in figure 3. Here the peak shift with electron energy is seen once again and finer

structure is revealed: for example at 20 keV, emission into the primary spectral peak at ~ 775 nm is concentrated in the backward direction between $\theta \sim 160^\circ$ and 180° , while longer wavelengths emerge at shallower angles. We anticipate that changes in angular emission profile, which may be measured in future experimental studies, will be associated with transitions between emission modes accessed under different pumping regimes.

Further to this, the BEM can generate maps of electromagnetic field intensity in and around the well structure, as shown in figure 4. It is interesting to note here that the field distribution corresponds to a guided cavity mode (to a first approximation it is cylindrically symmetric about the cavity axis) that is essentially independent of the radial electron injection coordinate r but strongly influenced by reflections at the two ends of the well (demonstrated by the axial intensity profile).

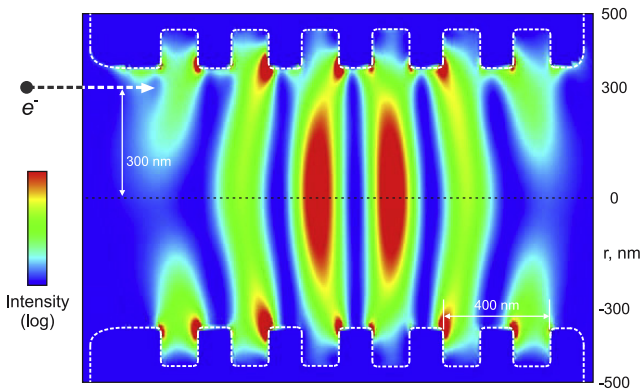


Figure 4. Cross-section showing the intensity $|E|^2$ of the electric field inside the light-well, calculated at the peak emission wavelength of 716 nm for a 40 keV electron injected (from the left) at $r = 300$ nm.

The uncertainty relation associated with the basic idea of emission via the creation of an oscillating dipole inside the well ($L\Delta\nu \sim \nu$, where ν is emission frequency and v is electron velocity [10]) indicates that emission line width will decrease with increasing well length L . This behavior is elegantly demonstrated by the boundary element model: figure 5(a) shows the evolution of the emission peak highlighted in figure 2(b) (where the number of periods $n = 6$, i.e. $L = 2.4 \mu\text{m}$) with well length.

Figure 5(b) shows the numerically modeled dependence of emission probability on the radial position of the electron injection point alongside the experimental dependence and analytical approximation presented in [10]. The BEM model matches the modified Bessel function approximation very well, with both predicting a rapid decay to zero emission for injection points more than ~ 100 nm from the wall of the well. In comparing these to the experimental result, which decays less rapidly and maintains a background emission level even at large distances, it should be noted that neither model accounts for the true electron beam diameter, or the fact that in experiment the electrons must ultimately collide with the sample (producing transition radiation even for axial trajectories).

The examples presented here show that boundary element modeling can reproduce all of the key characteristics observed experimentally in light-well emission. Ongoing analyses will help to optimize designs for future light-well structures and inform the development of experimental testing procedures. We anticipate that improvements in geometry, material composition and pumping regime will substantially enhance emission intensity and/or directionality: within the wider family of free-electron-driven radiators (including, for example, large-scale synchrotron undulators and free-electron lasers [19, 20]) substantial power outputs can, in the first instance, be achieved if the fields excited by the electrons interfere constructively. If the electron beam has sufficient time (path length) to interact with the emitted radiation then stimulated coherent emission (free-electron lasing) can occur. With appropriate structural and operational tuning, much brighter emission modes than have been observed so far should

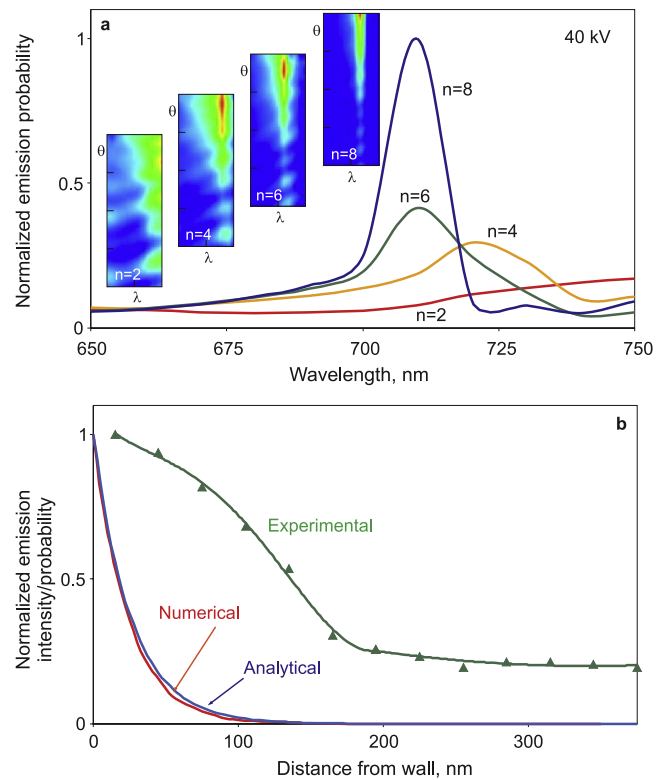


Figure 5. (a) Integrated emission probability ($\theta = 100^\circ\text{--}180^\circ$) as a function of wavelength for 40 keV electrons injected at a radius of 300 nm into wells of varying length, indicated by the number of periods n (as labeled). The insets show the emission probability as a function of wavelength λ from 650 to 750 nm and emission angle θ from 100° to 180° for each of the four cases. (b) BEM integrated emission probability ($n = 6$, red) as a function of the distance between electron injection point and the wall of the well alongside the experimentally measured 760 nm emission intensity (peak I in figure 1(c), green) and the analytically estimated emission probability (blue) for 40 keV electrons.

be accessible in light-wells, enabling them to offer tuneable, chip-scale light source functionality for nanophotonic circuit, optical memory and display applications.

Acknowledgments

The authors from the University of Southampton acknowledge the support of the UK Engineering and Physical Sciences Research Council (EPSRC, projects EP/C511786/1 and EP/F012810/1) and the European Union (FP6 project NMP4-2006-016881, ‘SPANS’). Those from the National Taiwan University thank the National Science Council of Taiwan (NSC-97-2120-M-002-013, NSC-97-2112-M-002-023-MY2 and NSC-97-2915-I-002-001) and the EPSRC (EP/F012810/1). Professor García de Abajo acknowledges the European Union (NMP4-2006-016881) and the Spanish MEC (MAT2007-66050 and Consolider ‘NanoLight.es’).

References

- [1] <http://nano.gov>
- [2] Nakamoto M 2008 *IEEE Industry Applications Society Annual Mtg (Edmonton, AB)* pp 447–51

- [3] Bashevoy M V, Jonsson F, Krasavin A V, Zheludev N I, Chen Y and Stockman M I 2006 *Nano Lett.* **6** 1113
- [4] van Wijngaarden J T, Verhagen E, Polman A, Ross C E, Lezec H J and Atwater H A 2006 *Appl. Phys. Lett.* **88** 221111
- [5] Bashevoy M V, Jonsson F, MacDonald K F and Zheludev N I 2007 *Opt. Express* **15** 11313
- [6] Vesseur E J R, de Waele R, Kuttge M and Polman A 2007 *Nano Lett.* **7** 2843
- [7] Nelayah J, Kociak M, Stéphan O, García de Abajo F J, Tencé M, Henrard L, Taverna D, Pastoriza-Santos I, Liz-Marzán L M and Colliex C 2007 *Nat. Phys.* **3** 348
- [8] Denisyuk A I, MacDonald K F, García de Abajo F J and Zheludev N I 2009 *Japan. J. Appl. Phys.* **48** 03A065
- [9] MacDonald K F, Adamo G, Zheludev N I, García de Abajo F J, Fu Y H, Wang C M and Tsai D P 2008 *Plasmonics and Metamaterials (META) 2008 (Rochester, NY)*
- [10] Adamo G, MacDonald K F, Fu Y H, Wang C-M, Tsai D P, García de Abajo F J and Zheludev N I 2009 *Phys. Rev. Lett.* **103** 113901
- [11] Koller D M, Hohenau A, Ditlbacher H, Galler N, Reil F, Aussenegg F R, Leitner A, List E J W and Krenn J R 2008 *Nat. Photon.* **2** 684
- [12] Hill M T *et al* 2007 *Nat. Photon.* **1** 589
- [13] Bergman D J and Stockman M I 2003 *Phys. Rev. Lett.* **90** 027402
- [14] Zheludev N I, Prosvirnin S L, Papasimakis N and Fedotov V A 2008 *Nat. Photon.* **2** 351
- [15] Park H-G, Barrelet C J, Wu Y, Tian B, Qian F and Lieber C M 2008 *Nat. Photon.* **2** 622
- [16] García de Abajo F J and Howie A 2002 *Phys. Rev. B* **65** 115418
- [17] Gómez-Medina R, Yamamoto N, Nakano M and García de Abajo F J 2008 *New J. Phys.* **10** 105009
- [18] Myroshnychenko V, Carbó-Argibay E, Pastoriza-Santos I, Pérez-Juste J, Liz-Marzán L M and García de Abajo F J 2008 *Adv. Mater.* **20** 4288
- [19] O'Shea P G and Freund H P 2001 *Science* **292** 1853
- [20] Gover A 2005 *Phys. Rev. Spec. Top. Accel. Beams* **8** 030701